Acta Cryst E CRYSTALLOGRAPHIC COMMUNICATIONS

ISSN 2056-9890

Crystal engineering of a 1:1 5-fluorocytosine–4-hydroxybenzaldehyde cocrystal: insights from X-ray crystallography and Hirshfeld analysis

Marimuthu Sangavi,[a] Marimuthu Mohana,[b]* Ray J. Butcher[c] and Colin D. McMillen[d]

[a]Department of Chemistry, Thanthai Periyar Government Arts and Science College, Tiruchirappalli-620 023, (Affiliated to Bharathidasan University, Tiruchirappalli 620 024, Tamil Nadu, India), Tamil Nadu, India, [b]Department of Chemistry, Periyar Maniammai Institute of Science and Technology (Deemed to be University), Thanjavur 613 403, Tamil Nadu, India, [c]Department of Chemistry, Howard University, Washington, DC 20059, USA, and [d]Department of Chemistry, Clemson University, H.L. Hunter Laboratories, Clemson, SC 29634, USA. *Correspondence e-mail: mmohana.chem@gmail.com

Received 25 April 2025
Accepted 17 May 2025

Edited by S.-L. Zheng, Harvard University, USA

Keywords: cocrystal; supramolecular network; dimeric motif; tetrameric motif; Hirshfeld surface analysis,fingerprint plots.

CCDC reference: 2452037

Supporting information: this article has supporting information at journals.iucr.org/e

The 1:1 cocrystal of 5-fluorocytosine (5FC) and 4-hydroxybenzaldehyde (4HB), $C_4H_4FN_3O{\cdot}C_7H_6O_2$ has been synthesized and its structure characterized by single-crystal X-ray diffraction and Hirshfeld surface analysis. The compound crystallizes in the monoclinic $P2_1/c$ space group. A robust supramolecular architecture is stabilized by N—H···O, N—H···N, C—H···O and C—H···F hydrogen bonds, forming $R_2^2(8)$, $R_4^4(22)$, $R_6^6(32)$, and $R_8^8(34)$ ring motifs. The N—H···O and N—H···N hydrogen bonds form strong directional interactions, contributing to the $R_2^2(8)$ and $R_8^8(34)$ motifs through dimeric and extended ring structures. O—H···O interactions link 5FC and 4HB molecules, generating an $R_6^6(32)$ ring that enhances the packing. Weaker C—H···F bonds help form the $R_4^4(22)$ tetrameric motif, supporting the overall three-dimensional supramolecular framework. Additionally, C—F···π interactions between the fluorine atom and the aromatic ring add further to the crystal cohesion. Hirshfeld surface analysis and two-dimensional fingerprint plots confirm that O···H/H···O contacts are the most significant, highlighting the central role of hydrogen bonding in the stability and organization of the crystal structure.

1. Chemical context

Cocrystals have gained considerable attention in supramolecular chemistry for their ability to improve the physical and chemical properties of active pharmaceutical ingredients (APIs) and functional materials without altering the molecular structure of the drug. They are defined as crystalline, single-phase solids composed of two or more distinct molecular and/or ionic compounds, typically in a stoichiometric ratio, which are neither simple salts nor solvates (Aitipamula *et al.*, 2012; Almarsson & Zaworotko, 2004). Cocrystals are stabilized through non-covalent interactions such as hydrogen bonding, π–π stacking, halogen bonding, and van der Waals forces. Their design is guided by the principles of crystal engineering, involving the careful selection of suitable coformers and the application of supramolecular synthons, such as the $R_2^2(8)$ hydrogen-bonded motif (Etter, 1990; Etter *et al.*, 1990; Desiraju, 1995). In the pharmaceutical industry, cocrystallization offers a promising strategy for enhancing the solubility, stability, and bioavailability of poorly soluble drugs. (Alvani & Shayanfar, 2022; Shi *et al.*, 2024). Compared to conventional techniques such as salt formation, micronization, solid dispersion, amorphous forms, and encapsulation, cocrystals offer the advantage of maintaining a stable crys-

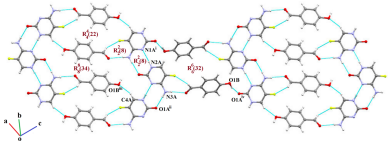

talline structure, which facilitates detailed characterization by X-ray diffraction (Bolla & Nangia, 2016; Bolla *et al.*, 2022).

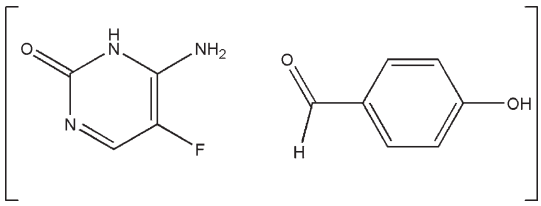

2. Structural commentary

Single-crystal X-ray diffraction analysis reveals that the title compound crystallizes in the monoclinic $P2_1/c$ space group with one molecule each of 5-fluorocytosine (5FC) and 4-hydroxybenzaldehyde (4HB) present in the asymmetric unit. An ellipsoid plot of the compound is shown in Fig. 1. Proton transfer does not occur between the hydroxyl group of benzaldehyde and the pyrimidine ring nitrogen atom of 5FC. The C—O bond length in the hydroxyl group of the 4HB molecule is 1.3520 (13) Å, with the corresponding internal bond angle [C2*A*—N1*A*—C3*A* = 120.00 (8)°] in agreement with reported literature values (Louis *et al.*, 1982; Mohana *et al.*, 2016, 2023; Sangavi *et al.*, 2024).

3. Supramolecular features and Hirshfeld surface analysis

The primary interaction motif is formed *via* N—H···O and C—H···F hydrogen bonds (Table 1). The N4*A* amino group and F1*A* atom of the 5FC molecule interact with the O2*B* and C7*B* atoms of the 4HB molecule, resulting in an $R_2^2(8)$ heterodimeric synthon. Heterodimers are further linked through a weak C—H···O^{iii} [symmetry code: (iii) $-x+2, -y+1, -z+1$] hydrogen bond involving the C4*A* atom of 5FC and the O1*B* atom of 4HB. The interaction leads to the formation of an $R_4^4(22)$ tetrameric synthon. The tetrameric motif is further extended through a homodimeric $R_2^2(8)$ synthon, formed by N—H···N^{i} [symmetry code: (i) $-x, y+\frac{1}{2}, -z+\frac{3}{2}$] and N—H···O^{ii} [symmetry code: (ii) $-x, y-\frac{1}{2}, -z+\frac{3}{2}$] hydrogen bonds. These interactions involve atoms N1*A*, N2*A*, N3*A* and O1*A* of the 5-fluorocytosine (5FC) molecule. The formation of this homodimeric synthon bridges adjacent tetrameric units, resulting in a large $R_8^8(34)$ ring motif. The alternating arrangement of $R_4^4(22)$ and $R_8^8(34)$ rings leads to the development of a three-dimensional supramolecular cage-like architecture. This network is further consolidated by O—H···O hydrogen-bonding interactions between the O1*A* atom of the 5FC molecule and the hydroxyl (–OH) group of the 4-hydroxybenzaldehyde (4HB) molecule. The hydrogen bonding occurs *via* an O—H···O^{iv} [symmetry code: (iv) $x+1, -y+\frac{1}{2}, z-\frac{1}{2}$] interaction, forming an $R_6^6(32)$ ring motif (Fig. 2). This interaction strengthens the packing and adds complexity to the supramolecular network. In addition to hydrogen bonding, the crystal structure is further consolidated by weak C—H···F and C—F···π interactions. The C—F···π interaction (Fig. 3) is observed between 5FC molecules [C1*A*···*Cg*^{v} = 3.2676 (9) Å, C1*A*—F1*A*···*Cg* = 89.41 (6)°, where *Cg* is the

Table 1
Hydrogen-bond geometry (Å, °).

D—H···*A*	*D*—H	H···*A*	*D*···*A*	*D*—H···*A*
N2*A*—H1···N1*A*^{i}	0.88 (1)	2.06 (1)	2.9354 (12)	175 (1)
N3*A*—H1*CC*···O2*B*	0.89 (1)	2.10 (1)	2.9848 (13)	170 (1)
N3*A*—H1*A*···O1*A*^{ii}	0.90 (1)	2.04 (1)	2.9328 (12)	176 (1)
C4*A*—H4*A*···O1*B*^{iii}	0.93	2.48	3.2905 (14)	145
O1*B*—H1*B*···O1*A*^{iv}	0.86 (2)	1.85 (2)	2.6934 (13)	166 (2)
C6*B*—H6*B*···F1*A*^{iii}	0.93	2.56	3.3446 (14)	143
C7*B*—H7*B*···F1*A*	0.93	2.51	2.9886 (14)	112

Symmetry codes: (i) $-x, y+\frac{1}{2}, -z+\frac{3}{2}$; (ii) $-x, y-\frac{1}{2}, -z+\frac{3}{2}$; (iii) $-x+2, -y+1, -z+1$; (iv) $x+1, -y+\frac{1}{2}, z-\frac{1}{2}$.

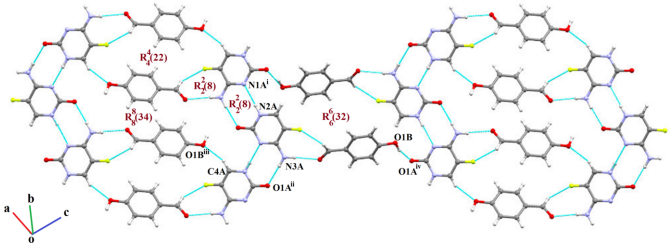

Figure 2
Three-dimensional supramolecular cage-like architecture formed *via* N—H···O, N—H···N, O—H···O, C—H···F and C—H···O hydrogen bonds. [Symmetry codes: (i) $-x, y+\frac{1}{2}, -z+\frac{3}{2}$; (ii) $-x, y-\frac{1}{2}, -z+\frac{3}{2}$; (iii) $-x+2, -y+1, -z+1$; (iv) $x+1, -y+\frac{1}{2}, z-\frac{1}{2}$.]

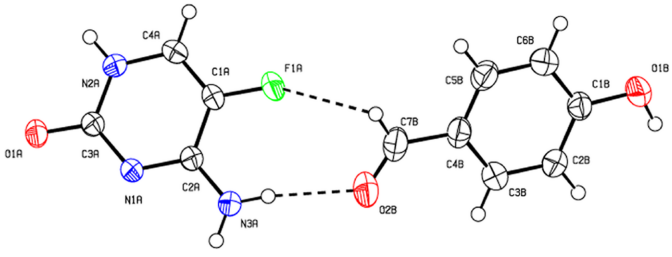

Figure 1
The molecular structure of the title cocrystal with displacement ellipsoids drawn at the 50% probability level. Hydrogen bonds are shown as dashed lines.

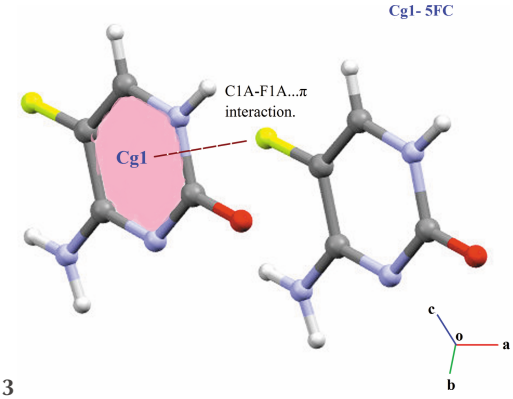

Figure 3
A view of the C—F···π interaction (symmetry operation $1+x, y, z$).

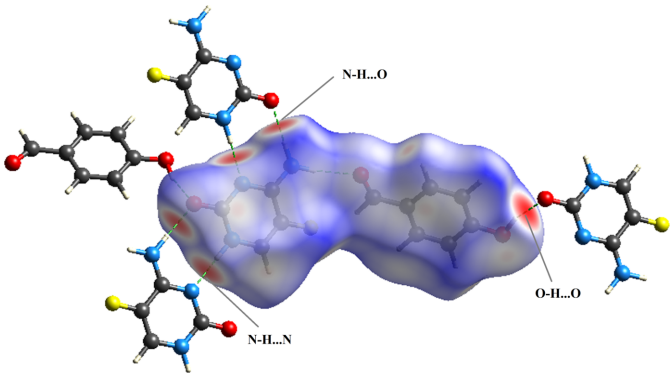

Figure 4
The Hirshfeld surface mapped over d_{norm} showing the N—H···O, N—H···N and O—H···O interactions as dashed gray lines.

centroid of the 5FC ring; symmetry code: (v) 1 + x, y, z]. The observed angle is consistent with values reported in the literature (Sikorski *et al.*, 2005; Vangala *et al.*, 2002).

Hirshfeld surface (HS) analysis was performed for the title compound to visualize and quantify its intermolecular interactions. Fig. 4 presents the van der Waals interactions using a Hirshfeld surface mapped over d_{norm} (Spackman & Jayatilaka, 2009), generated with *Crystal Explorer 21* (Spackman *et al.*, 2021). This analysis reveals significant intermolecular hydrogen bonds of the types N—H···O, N—H···N and O—H···O interactions. In the surface representation, red areas indicate strong hydrogen bonding, blue regions correspond to contacts close to the sum of the van der Waals radii, and white regions represent weaker interactions.

To analyze the relative contributions of different intermolecular interactions, two-dimensional fingerprint plots were generated (McKinnon *et al.*, 2007) and these are shown in Fig. 5. These plots indicate that the most prominent contacts are O···H/H···O (26.6%), followed by H···H (25.5%), C···H/H···C (16.7%), N···H/H···N (10.0%) and F···H/H···F (6.2%). The crystallographic analysis reveals a robust supramolecular network in the title compound, stabilized by hydrogen bonds (N—H···O, N—H···N, O—H···O and C—H···F) and C—F···π interactions, forming a three-dimensional cage-like supramolecular architecture. Hirshfeld surface analysis highlights prominent O···H/H···O interactions, alongside other significant contacts, contributing to crystal stability. The study demonstrates how non-covalent interactions, including hydrogen-bonding and π interactions, govern the molecular packing and cohesion, supporting the principles of supramolecular chemistry in crystal engineering.

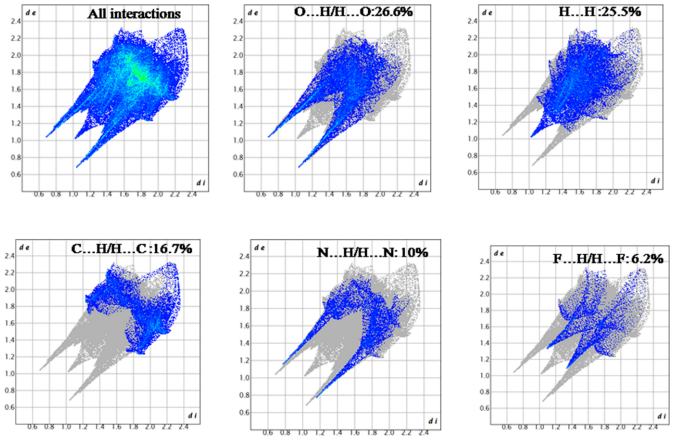

Figure 5
Fingerprint plots showing the total contribution of individual interactions and those delineated into O···H/H···O, H···H, C···H/H···C, N···H/H···N and F···H/H···F interactions.

4. Database survey

5-Fluorocytosine (5FC) is a synthetic antimycotic compound, first synthesized in 1957 and widely used as an antitumor agent. It is also active against fungal infection (Portalone & Colapietro, 2007; Vermes *et al.*, 2000). It becomes active by deamination of 5FC into 5-fluorouracil by the enzyme cytosine deaminase (CD) and inhibits RNA and DNA synthesis (Morschhauser, 2003). The Cambridge Structural Database (CSD, v5.45, June 2024; Groom *et al.*, 2016) reference codes for the monohydrate are BIRMEU, BIRMEU01, BIRMEU02, BIRMEU03, MEBQUG, MEBQIU, MEBQOA and GATMUL (Louis *et al.*, 1982; Portalone & Colapietro, 2006; Hulme & Tocher, 2006; Portalone, 2011), and for the polymorphs: DUKWIQ, DUKWAI and DUKWEM (Tutughamiarso *et al.*, 2009). A wide range of cocrystals has also been documented, such as XOQQUS, MECTUL, MECVEX, MECVIB, MECVOH, MECVUN, MECWAU, MECWEY, MECWOI, MECWUO, MECXEZ, MECXID, MECXOJ, GIFWIF, UJUJAM, and POCWUD (Souza *et al.*, 2019; Tutughamiarso *et al.*, 2012; Tutughamiarso & Egert, 2012; Mohana *et al.*, 2016, 2023; Sangavi *et al.*, 2024). Salts include WEWZAA01, SIJXAM, SIJXIU, SIJXUG, EDATOS, GIFWEB, POCXAK, ZAPFEE and ROLTUJ WEWZAA01, SIJXAM, SIJXIU, SIJXUG, EDATOS, GIFWEB, POCXAK, ZAPFEE and ROLTUJ (Perumalla *et al.*, 2013*a*,*b*; Prabakaran *et al.*, 2001; Mohana *et al.*, 2017; Karthikeyan *et al.*, 2014) have been reported in the literature. 4-Hydroxybenzaldehydes are potential therapeutic agents for the treatment of human angiostrongyliasis. The crystal structure of 4-hydroxybenzaldehyde (Jasinski *et al.*, 2008), as well as its cocrystal (Nowak & Sikorski, 2023) and polymorphic forms (Simões *et al.*, 2013) have also been reported. 5FC contains multiple hydrogen-bond donors and acceptors, including amino and carbonyl groups, and 4-HBA offers hydroxyl and aldehyde functionalities capable of forming hydrogen bonds, along with an aromatic ring that can engage in π–π interactions. The present work focuses on the supramolecular hydrogen bonding interactions in the crystal structure of 1:1 cocrystals of 5-fluorocytosine-4-hydroxybenzaldehyde.

5. Synthesis and crystallization

The title compound was synthesized by mixing a hot ethanolic solution of 5-fluorocytosine with 4-hydroxybenzaldehyde in a

Table 2
Experimental details.

Crystal data	
Chemical formula	$C_4H_4FN_3O{\cdot}C_7H_6O_2$
M_r	251.22
Crystal system, space group	Monoclinic, $P2_1/c$
Temperature (K)	297
a, b, c (Å)	4.2126 (1), 9.6687 (1), 26.8628 (5)
β (°)	94.186 (1)
V (Å^3)	1091.21 (3)
Z	4
Radiation type	Cu $K\alpha$
μ (mm^{-1})	1.07
Crystal size (mm)	0.27 × 0.21 × 0.17
Data collection	
Diffractometer	XtaLAB Synergy, Dualflex, HyPix
Absorption correction	Analytical (*CrysAlis PRO*; Rigaku OD, 2023)
T_{min}, T_{max}	0.782, 0.840
No. of measured, independent and observed [$I > 2\sigma(I)$] reflections	19824, 2243, 2127
R_{int}	0.019
(sin $\theta/\lambda)_{max}$ (Å^{-1})	0.630
Refinement	
$R[F^2 > 2\sigma(F^2)]$, $wR(F^2)$, S	0.034, 0.101, 1.04
No. of reflections	2243
No. of parameters	180
No. of restraints	4
H-atom treatment	H atoms treated by a mixture of independent and constrained refinement
$\Delta\rho_{max}$, $\Delta\rho_{min}$ (e Å^{-3})	0.20, −0.19

Computer programs: *CrysAlis PRO* (Rigaku OD, 2023), *SHELXT* (Sheldrick, 2015*a*), *SHELXL2019/2* (Sheldrick, 2015*b*), *PLATON* (Spek, 2020), *Mercury* (Macrae *et al.*, 2020), *POVRay* (Cason, 2004) and *publCIF* (Westrip, 2010).

1:1 molar ratio. The solution was heated in a water bath at 333 K for 30 minutes and then allowed to cool slowly to room temperature. After a few days, colorless crystals had separated out of the mother liquor.

6. Refinement

Crystal data, data collection and structure refinement details are summarized in Table 2. The H atoms of the N—H, –NH_2 and OH groups were located in difference-Fourier maps and refined freely. Other H atoms were placed geometrically (C—H = 0.93 Å) and refined using a riding model with U_{iso}(H) = 1.2U_{eq}(C).

Funding information

We thank Howard University and the National Science Foundation Major Research Instrumentation program (NSF DMR-2117502) for financially supporting the acquisition of the Rigaku Synergy single-crystal X-ray diffractometer used in this study.

References

Aitipamula, S., Banerjee, R., Bansal, A. K., Biradha, K., Cheney, M. L., Choudhury, A. R., Desiraju, G. R., Dikundwar, A. G., Dubey, R., Duggirala, N., Ghogale, P. P., Ghosh, S., Goswami, P. K., Goud, N. R., Jetti, R. R. K. R., Karpinski, P., Kaushik, P., Kumar, D., Kumar, V., Moulton, B., Mukherjee, A., Mukherjee, G., Myerson, A. S., Puri, V., Ramanan, A., Rajamannar, T., Reddy, C. M., Rodriguez-Hornedo, N., Rogers, R. D., Row, T. N. G., Sanphui, P., Shan, N., Shete, G., Singh, A., Sun, C. C., Swift, J. A., Thaimattam, R., Thakur, T. S., Kumar Thaper, R., Thomas, S. P., Tothadi, S., Vangala, V. R., Variankaval, N., Vishweshwar, P., Weyna, D. R. & Zaworotko, M. J. (2012). *Cryst. Growth Des.* **12**, 2147–2152.

Almarsson, O. & Zaworotko, M. J. (2004). *Chem. Commun.* pp. 1889–1896.

Alvani, A. & Shayanfar, A. (2022). *Cryst. Growth Des.* **22**, 6323–6337.

Bolla, G. & Nangia, A. (2016). *Chem. Commun.* **52**, 8342–8360.

Bolla, G., Sarma, B. & Nangia, A. K. (2022). *Chem. Rev.* **122**, 11514–11603.

Cason, C. J. (2004). *POV-RAY for Windows.* Persistence of Vision Raytracer Pvt Ltd, Victoria, Australia. http://www.povray.org

Desiraju, G. R. (1995). *Angew. Chem. Int. Ed. Engl.* **34**, 2311–2327.

Etter, M. C. (1990). *Acc. Chem. Res.* **23**, 120–126.

Etter, M. C., Urbanczyk-Lipkowska, Z., Zia-Ebrahimi, M. & Panunto, T. W. (1990). *J. Am. Chem. Soc.* **112**, 8415–8426.

Groom, C. R., Bruno, I. J., Lightfoot, M. P. & Ward, S. C. (2016). *Acta Cryst.* B**72**, 171–179.

Hulme, A. T. & Tocher, D. A. (2006). *Cryst. Growth Des.* **6**, 481–487.

Jasinski, J. P., Butcher, R. J., Narayana, B., Swamy, M. T. & Yathirajan, H. S. (2008). *Acta Cryst.* E**64**, o187.

Karthikeyan, A., Thomas Muthiah, P. & Perdih, F. (2014). *Acta Cryst.* E**70**, 328–330.

Louis, T., Low, J. N. & Tollin, P. (1982). *Cryst. Struct. Commun.* **11**, 1059–1064.

Macrae, C. F., Sovago, I., Cottrell, S. J., Galek, P. T. A., McCabe, P., Pidcock, E., Platings, M., Shields, G. P., Stevens, J. S., Towler, M. & Wood, P. A. (2020). *J. Appl. Cryst.* **53**, 226–235.

McKinnon, J. J., Jayatilaka, D. & Spackman, M. A. (2007). *Chem. Commun.* pp. 3814–3816.

Mohana, M., Muthiah, P. T., Sanjeewa, L. D. & McMillen, C. D. (2016). *Acta Cryst.* E**72**, 552–555.

Mohana, M., Thomas Muthiah, P. & McMillen, C. D. (2017). *Acta Cryst.* E**73**, 361–364.

Mohana, M., Thomas Muthiah, P., McMillen, C. D. & Butcher, R. J. (2023). *Acta Cryst.* C**79**, 61–67.

Morschhäuser, J. (2003). *Pharm. Unserer Zeit* **32**, 124–129.

Nowak, P. & Sikorski, A. (2023). *RSC Adv.* **13**, 20105–20112.

Perumalla, S. R., Pedireddi, V. R. & Sun, C. C. (2013*a*). *Cryst. Growth Des.* **13**, 429–432.

Perumalla, S. R., Pedireddi, V. R. & Sun, C. C. (2013*b*). *Mol. Pharm.* **10**, 2462–2466.

Portalone, G. (2011). *Chem. Cent. J.* **5**, 51.

Portalone, G. & Colapietro, M. (2006). *Acta Cryst.* E**62**, o1049–o1051.

Portalone, G. & Colapietro, M. (2007). *J. Chem. Crystallogr.* **37**, 141–145.

Prabakaran, P., Murugesan, S., Muthiah, P. T., Bocelli, G. & Righi, L. (2001). *Acta Cryst.* E**57**, o933–o936.

Rigaku OD. (2023). *CrysAlis PRO.* Rigaku Oxford Diffraction Ltd, Yarnton, England.

Sangavi, M., Kumaraguru, N., Butcher, R. J. & McMillen, C. D. (2024). *Acta Cryst.* C**80**, 30–36.

Sheldrick, G. M. (2015*a*). *Acta Cryst.* C**71**, 3–8.

Sheldrick, G. M. (2015*b*). *Acta Cryst.* A**71**, 3–8.

Shi, J., Zhang, Y., An, Q., Li, Y. & Liu, L. (2024). *J. Solid State Chem.* **331**, 124545.

Sikorski, A., Krzymiński, K., Niziołek, A. & Błażejowski, J. (2005). *Acta Cryst.* C**61**, o690–o694.

Simões, R. G., Bernardes, C. E. S. & da Piedade, M. E. M. (2013). *Cryst. Growth Des.* **13**, 2803–2814.

Souza, M. S., Diniz, L. F., Alvarez, N., da Silva, C. C. P. & Ellena, J. (2019). *New J. Chem.* **43**, 15924–15934.

Spackman, M. A. & Jayatilaka, D. (2009). *CrystEngComm* **11**, 19–32.

Spackman, P. R., Turner, M. J., McKinnon, J. J., Wolff, S. K., Grimwood, D. J., Jayatilaka, D. & Spackman, M. A. (2021). *J. Appl. Cryst.* **54**, 1006–1011.
Spek, A. L. (2020). *Acta Cryst.* E**76**, 1–11.
Tutughamiarso, M. & Egert, E. (2012). *Acta Cryst*. B**68**, 444–452
Tutughamiarso, M., Bolte, M. & Egert, E. (2009). *Acta Cryst.* C**65**, o574–o578.
Tutughamiarso, M., Wagner, G. & Egert, E. (2012). *Acta Cryst.* B**68**, 431–443.
Vangala, V. R., Nangia, A. & Lynch, D. E. (2002). *Chem. Commun.* pp. 1304–1305.
Vermes, A., Guchelaar, H. J. & Dankert, J. (2000). *J. Antimicrob. Chemother.* **46**, 171–179.
Westrip, S. P. (2010). *J. Appl. Cryst.* **43**, 920–925.

supporting information

Acta Cryst. (2025). E**81**, 549-553 [https://doi.org/10.1107/S2056989025004463]

Crystal engineering of a 1:1 5-fluorocytosine–4-hydroxybenzaldehyde cocrystal: insights from X-ray crystallography and Hirshfeld analysis

Marimuthu Sangavi, Marimuthu Mohana, Ray J. Butcher and Colin D. McMillen

Computing details

4-Amino-5-fluoro-1*H*-pyrimidin-2-one–4-hydroxybenzaldehyde (1/1)

Crystal data

$C_4H_4FN_3O·C_7H_6O_2$
M_r = 251.22
Monoclinic, $P2_1/c$
a = 4.2126 (1) Å
b = 9.6687 (1) Å
c = 26.8628 (5) Å
β = 94.186 (1)°
V = 1091.21 (3) Å^3
Z = 4
$F(000)$ = 520
D_x = 1.529 Mg m^{-3}
Cu $K\alpha$ radiation, λ = 1.54184 Å
Cell parameters from 18043 reflections
θ = 3.3–76.2°
μ = 1.07 mm^{-1}
T = 297 K
Block, colorless
0.27 × 0.21 × 0.17 mm

Data collection

XtaLAB Synergy, Dualflex, HyPix diffractometer
Radiation source: micro-focus sealed X-ray tube
Detector resolution: 10.0000 pixels mm^{-1}
ω scans
Absorption correction: analytical (CrysAlisPro; Rigaku OD, 2023)
T_{min} = 0.782, T_{max} = 0.840
19824 measured reflections
2243 independent reflections
2127 reflections with $I > 2\sigma(I)$
R_{int} = 0.019
θ_{max} = 76.2°, θ_{min} = 3.3°
h = −3→5
k = −12→12
l = −33→33

Refinement

Refinement on F^2
Least-squares matrix: full
$R[F^2 > 2\sigma(F^2)]$ = 0.034
$wR(F^2)$ = 0.101
S = 1.04
2243 reflections
180 parameters
4 restraints
Primary atom site location: dual
Secondary atom site location: difference Fourier map
Hydrogen site location: mixed
H atoms treated by a mixture of independent and constrained refinement
$w = 1/[\sigma^2(F_o^2) + (0.0563P)^2 + 0.2241P]$ where $P = (F_o^2 + 2F_c^2)/3$
$(\Delta/\sigma)_{max}$ = 0.001
$\Delta\rho_{max}$ = 0.20 e Å^{-3}
$\Delta\rho_{min}$ = −0.19 e Å^{-3}
Extinction correction: *SHELXL2019/2* (Sheldrick, 2015b), $Fc^*=kFc[1+0.001xFc^2\lambda^3/\sin(2\theta)]^{-1/4}$
Extinction coefficient: 0.0088 (13)

Special details

Geometry. All esds (except the esd in the dihedral angle between two l.s. planes) are estimated using the full covariance matrix. The cell esds are taken into account individually in the estimation of esds in distances, angles and torsion angles; correlations between esds in cell parameters are only used when they are defined by crystal symmetry. An approximate (isotropic) treatment of cell esds is used for estimating esds involving l.s. planes.

Refinement. The data collection, cell refinement, and data reduction were performed using CrysAlisPro (Rigaku OD, 2023). Structure solution was carried out with SHELXT 2014/5 (Sheldrick, 2015a) and refinement was done using SHELXL-2016/6 (Sheldrick, 2015b). Molecular graphics were prepared using PLATON (Spek, 2020), Mercury (Macrae *et al.*, 2020) and POVRay (Cason 2004).

Fractional atomic coordinates and isotropic or equivalent isotropic displacement parameters (Å²)

	x	*y*	*z*	U_{iso}*/U_{eq}
F1A	0.6004 (2)	0.39753 (7)	0.63425 (3)	0.0557 (2)
O1A	−0.1067 (2)	0.40145 (8)	0.79019 (3)	0.0439 (2)
N1A	0.1299 (2)	0.27556 (9)	0.73165 (3)	0.0331 (2)
N2A	0.1501 (2)	0.51932 (9)	0.73260 (3)	0.0344 (2)
H1	0.076 (3)	0.5966 (14)	0.7444 (6)	0.050 (4)*
N3A	0.3795 (3)	0.15570 (10)	0.67141 (4)	0.0401 (3)
H1CC	0.492 (3)	0.1523 (16)	0.6446 (5)	0.049 (4)*
H1A	0.294 (3)	0.0798 (14)	0.6845 (5)	0.045 (4)*
C1A	0.4154 (3)	0.40215 (11)	0.67318 (4)	0.0351 (3)
C2A	0.3072 (2)	0.27452 (11)	0.69223 (4)	0.0313 (2)
C3A	0.0531 (2)	0.39737 (10)	0.75270 (4)	0.0323 (2)
C4A	0.3331 (3)	0.52236 (11)	0.69305 (4)	0.0356 (3)
H4A	0.399417	0.605918	0.680151	0.043*
O1B	1.1638 (2)	0.27251 (10)	0.35919 (3)	0.0520 (3)
H1B	1.074 (4)	0.2080 (18)	0.3414 (7)	0.076 (5)*
O2B	0.6793 (3)	0.13585 (11)	0.57435 (3)	0.0605 (3)
C1B	1.0816 (3)	0.25581 (12)	0.40653 (4)	0.0383 (3)
C2B	0.8831 (3)	0.14938 (12)	0.42006 (4)	0.0421 (3)
H2B	0.798860	0.087622	0.396053	0.050*
C3B	0.8117 (3)	0.13552 (13)	0.46892 (4)	0.0450 (3)
H3B	0.677170	0.064757	0.477749	0.054*
C4B	0.9386 (3)	0.22637 (12)	0.50533 (4)	0.0401 (3)
C5B	1.1361 (3)	0.33238 (13)	0.49140 (4)	0.0440 (3)
H5B	1.222274	0.393527	0.515464	0.053*
C6B	1.2064 (3)	0.34827 (13)	0.44238 (5)	0.0471 (3)
H6B	1.336473	0.420430	0.433386	0.056*
C7B	0.8656 (3)	0.21566 (14)	0.55746 (4)	0.0474 (3)
H7B	0.972343	0.275878	0.579901	0.057*

Atomic displacement parameters (Å²)

	U^{11}	U^{22}	U^{33}	U^{12}	U^{13}	U^{23}
F1A	0.0776 (5)	0.0414 (4)	0.0534 (5)	−0.0025 (3)	0.0416 (4)	0.0020 (3)
O1A	0.0648 (5)	0.0344 (4)	0.0352 (4)	0.0058 (4)	0.0229 (4)	0.0028 (3)
N1A	0.0453 (5)	0.0265 (4)	0.0287 (4)	−0.0013 (3)	0.0106 (4)	0.0013 (3)
N2A	0.0456 (5)	0.0250 (4)	0.0338 (5)	0.0007 (3)	0.0103 (4)	−0.0009 (3)

N3A	0.0588 (6)	0.0295 (5)	0.0341 (5)	−0.0013 (4)	0.0177 (4)	−0.0018 (4)
C1A	0.0421 (6)	0.0337 (6)	0.0310 (5)	−0.0024 (4)	0.0131 (4)	0.0025 (4)
C2A	0.0383 (5)	0.0296 (5)	0.0265 (5)	−0.0006 (4)	0.0053 (4)	0.0009 (4)
C3A	0.0416 (5)	0.0285 (5)	0.0274 (5)	0.0006 (4)	0.0065 (4)	0.0018 (4)
C4A	0.0423 (6)	0.0290 (5)	0.0364 (5)	−0.0035 (4)	0.0096 (4)	0.0047 (4)
O1B	0.0734 (6)	0.0513 (5)	0.0327 (4)	−0.0134 (4)	0.0137 (4)	0.0001 (4)
O2B	0.0838 (7)	0.0605 (6)	0.0404 (5)	0.0017 (5)	0.0255 (5)	0.0006 (4)
C1B	0.0477 (6)	0.0370 (5)	0.0311 (5)	0.0040 (4)	0.0082 (4)	0.0018 (4)
C2B	0.0536 (7)	0.0389 (6)	0.0343 (6)	−0.0031 (5)	0.0075 (5)	−0.0055 (4)
C3B	0.0549 (7)	0.0419 (6)	0.0397 (6)	−0.0053 (5)	0.0140 (5)	−0.0004 (5)
C4B	0.0464 (6)	0.0422 (6)	0.0324 (5)	0.0101 (5)	0.0080 (4)	−0.0005 (4)
C5B	0.0528 (7)	0.0425 (6)	0.0367 (6)	0.0017 (5)	0.0026 (5)	−0.0072 (5)
C6B	0.0595 (7)	0.0406 (6)	0.0418 (6)	−0.0090 (5)	0.0083 (5)	−0.0015 (5)
C7B	0.0569 (7)	0.0521 (7)	0.0342 (6)	0.0110 (6)	0.0102 (5)	−0.0031 (5)

Geometric parameters (Å, º)

F1A—C1A	1.3498 (12)	O1B—H1B	0.857 (15)
O1A—C3A	1.2521 (13)	O2B—C7B	1.2122 (17)
N1A—C2A	1.3397 (13)	C1B—C6B	1.3889 (17)
N1A—C3A	1.3558 (13)	C1B—C2B	1.3907 (16)
N2A—C4A	1.3578 (14)	C2B—C3B	1.3746 (16)
N2A—C3A	1.3715 (13)	C2B—H2B	0.9300
N2A—H1	0.877 (13)	C3B—C4B	1.3920 (17)
N3A—C2A	1.3231 (14)	C3B—H3B	0.9300
N3A—H1CC	0.891 (13)	C4B—C5B	1.3887 (18)
N3A—H1A	0.900 (12)	C4B—C7B	1.4594 (15)
C1A—C4A	1.3353 (15)	C5B—C6B	1.3791 (17)
C1A—C2A	1.4235 (14)	C5B—H5B	0.9300
C4A—H4A	0.9300	C6B—H6B	0.9300
O1B—C1B	1.3520 (13)	C7B—H7B	0.9300
C2A—N1A—C3A	120.00 (8)	O1B—C1B—C2B	122.30 (10)
C4A—N2A—C3A	121.95 (9)	C6B—C1B—C2B	119.97 (10)
C4A—N2A—H1	120.1 (10)	C3B—C2B—C1B	119.96 (11)
C3A—N2A—H1	117.8 (10)	C3B—C2B—H2B	120.0
C2A—N3A—H1CC	121.8 (10)	C1B—C2B—H2B	120.0
C2A—N3A—H1A	115.6 (9)	C2B—C3B—C4B	120.64 (11)
H1CC—N3A—H1A	122.4 (14)	C2B—C3B—H3B	119.7
C4A—C1A—F1A	121.33 (9)	C4B—C3B—H3B	119.7
C4A—C1A—C2A	120.77 (10)	C5B—C4B—C3B	118.92 (10)
F1A—C1A—C2A	117.90 (9)	C5B—C4B—C7B	118.91 (11)
N3A—C2A—N1A	119.97 (9)	C3B—C4B—C7B	122.16 (11)
N3A—C2A—C1A	120.74 (9)	C6B—C5B—C4B	120.93 (11)
N1A—C2A—C1A	119.29 (9)	C6B—C5B—H5B	119.5
O1A—C3A—N1A	121.43 (9)	C4B—C5B—H5B	119.5
O1A—C3A—N2A	118.86 (9)	C5B—C6B—C1B	119.58 (11)
N1A—C3A—N2A	119.71 (9)	C5B—C6B—H6B	120.2

C1A—C4A—N2A	118.21 (9)	C1B—C6B—H6B	120.2
C1A—C4A—H4A	120.9	O2B—C7B—C4B	126.30 (12)
N2A—C4A—H4A	120.9	O2B—C7B—H7B	116.9
C1B—O1B—H1B	107.7 (13)	C4B—C7B—H7B	116.9
O1B—C1B—C6B	117.73 (11)		
C3A—N1A—C2A—N3A	−179.36 (10)	O1B—C1B—C2B—C3B	178.79 (11)
C3A—N1A—C2A—C1A	0.55 (16)	C6B—C1B—C2B—C3B	−0.23 (19)
C4A—C1A—C2A—N3A	177.61 (11)	C1B—C2B—C3B—C4B	−0.64 (19)
F1A—C1A—C2A—N3A	−1.78 (16)	C2B—C3B—C4B—C5B	0.72 (18)
C4A—C1A—C2A—N1A	−2.30 (17)	C2B—C3B—C4B—C7B	179.39 (11)
F1A—C1A—C2A—N1A	178.31 (9)	C3B—C4B—C5B—C6B	0.07 (18)
C2A—N1A—C3A—O1A	−178.50 (10)	C7B—C4B—C5B—C6B	−178.65 (11)
C2A—N1A—C3A—N2A	1.84 (16)	C4B—C5B—C6B—C1B	−0.9 (2)
C4A—N2A—C3A—O1A	177.67 (10)	O1B—C1B—C6B—C5B	−178.06 (11)
C4A—N2A—C3A—N1A	−2.66 (16)	C2B—C1B—C6B—C5B	1.01 (19)
F1A—C1A—C4A—N2A	−179.10 (9)	C5B—C4B—C7B—O2B	173.98 (12)
C2A—C1A—C4A—N2A	1.53 (17)	C3B—C4B—C7B—O2B	−4.7 (2)
C3A—N2A—C4A—C1A	0.92 (17)		

Hydrogen-bond geometry (Å, º)

D—H···*A*	*D*—H	H···*A*	*D*···*A*	*D*—H···*A*
N2*A*—H1···N1*A*^{i}	0.88 (1)	2.06 (1)	2.9354 (12)	175 (1)
N3*A*—H1*CC*···O2*B*	0.89 (1)	2.10 (1)	2.9848 (13)	170 (1)
N3*A*—H1*A*···O1*A*^{ii}	0.90 (1)	2.04 (1)	2.9328 (12)	176 (1)
C4*A*—H4*A*···O1*B*^{iii}	0.93	2.48	3.2905 (14)	145
O1*B*—H1*B*···O1*A*^{iv}	0.86 (2)	1.85 (2)	2.6934 (13)	166 (2)
C6*B*—H6*B*···F1*A*^{iii}	0.93	2.56	3.3446 (14)	143
C7*B*—H7*B*···F1*A*	0.93	2.51	2.9886 (14)	112

Symmetry codes: (i) −*x*, *y*+1/2, −*z*+3/2; (ii) −*x*, *y*−1/2, −*z*+3/2; (iii) −*x*+2, −*y*+1, −*z*+1; (iv) *x*+1, −*y*+1/2, *z*−1/2.